minerals

MDPI

Article

Kinetic Study in Atmospheric Pressure Organic Acid Leaching: Shrinking Core Model versus Lump Model

Kevin Cleary Wanta [1], Widi Astuti [2], Indra Perdana [3] and Himawan Tri Bayu Murti Petrus [3,4,*]

[1] Department of Chemical Engineering, Faculty of Industrial Technology, Parahyangan Catholic University, Bandung 40141, Indonesia; kcwanta@unpar.ac.id

[2] Research Unit for Mineral Technology, Indonesian Institute of Sciences (LIPI), Tanjung Bintang 35361, Indonesia; widi.mineral@gmail.com

[3] Department of Chemical Engineering (Sustainable Mineral Processing Research Group), Faculty of Engineering, Universitas Gadjah Mada, Yogyakarta 55281, Indonesia; iperdana@ugm.ac.id

[4] Unconventional Geo-resources Research Group, Faculty of Engineering, Universitas Gadjah Mada, Yogyakarta 55281, Indonesia

* Correspondence: bayupetrus@ugm.ac.id; Tel.: +62-274-555320

Received: 26 May 2020; Accepted: 3 July 2020; Published: 9 July 2020

Abstract: The kinetics study has an essential role in the scale-up process because it illustrates the real phenomena of a process. This study aims to develop a mathematical model that can explain the mechanism of the leaching process of laterite ore using a low concentration of the citric acid solution and evaluate that model using the experimental data. As a raw material, this process used powder-shaped limonite laterite ores with a size of 125–150 μm. The leaching process is carried out using 0.1 M citric acid solution, F:S ratio of 1:20, and a leaching time of 2 h. The temperature parameter was varied at 303, 333, and 358 K. The experimental results showed that the higher the operating temperature, the higher the extracted nickel. The results of this experiment were used to evaluate the shrinking core kinetics model and the lumped model. The simulation results for both models show that the lumped model can provide better simulation results. Quantitatively, the percentage of errors from the shrinking core model is around 3.5 times greater than the percentage of errors from using the lumped model. This result shows that in this leaching process, the process mechanism that occurs involves the reactant diffusion step and the chemical reactions step; those steps run simultaneously.

Keywords: citric acid; kinetics; leaching; lump model; nickel laterite; shrinking core model

1. Introduction

It is undeniable that energy is one of the most important things that affect human survival. Over the years, the fulfilment of energy demand derives from fossil fuels, which are categorized as conventional or non-renewable energy [1,2]. Consequently, this kind of energy will reach its scarcity phase if people use this energy continuously. This condition forces researchers to develop various renewable energy technologies, such as rechargeable batteries [3–7]. Rechargeable batteries are electrical batteries that can be recharged many times; they can be defined as an energy storage system. Various electronic devices, such as electric vehicles and portable electronics, apply this type of battery as a source of energy [8,9].

In rechargeable battery technology, electrode components have an essential role. This kind of battery uses metal-based compounds as electrodes. For example, nickel-based rechargeable batteries, like nickel-cadmium (NiCd), nickel-metal hydride (NiMH), and nickel-hydrogen (NiH_2), use nickel-based compounds, such as nickel oxide (NiO), nickel hydroxide ($Ni(OH)_2$) or nickel sulphide (NiS) as cathode material [10–12]. The production of rechargeable batteries must use high purity compounds. The synthesis of these compounds undergoes various critical processes, and one of them is the hydrometallurgy process.

Hydrometallurgy, usually called the leaching process, is a process of extracting metal ions from the mineral resources, both primary and secondary resources, using a solvent [13]. This process is one of the initial steps of producing rechargeable batteries. It provides a precursor solution as raw material for synthesizing high purity electrode materials. As a result, when the production of the batteries is accelerating, the supply of the precursor solution also rapidly increases, and it has to be developed on an industrial scale. The scale-up process from laboratory scale to industrial scale will also cause a change in process equipment dimensions, especially the extractor unit, which must follow its kinetics model. The process kinetics show the real process phenomenon happens in the extractor. Consequently, the extraction results at the industrial scale are the same as the results of the laboratory.

Based on previous studies, the shrinking core model is considered as the most suitable to describe the kinetics model for the leaching process of metal ions [14–21]. The leaching process is a heterogeneous process that involves several fundamental steps that are simultaneously involved and affect each other. Those steps are the diffusion step through the liquid film layer, the diffusion step in solid, and a chemical reaction step. However, in utilizing the shrinking core model in the leaching process, there is only one step that controls the process, namely the step at the slowest rate. This condition raises questions and doubts related to a process that can consist of several steps, but only one step is considered to control the process in the kinetics study of the process. As evidence and consideration, our other results indicate that the shrinking core model was not suitable for using an organic solvent in the leaching process [22].

In this study, we devised a mathematical equation that is able to illustrate the real physical phenomena of the leaching process. This mathematical model is derived from the modification of the shrinking core model, where all steps of the leaching process involved are calculated. These steps are considered as resistance, which behave simultaneously in the leaching process. Therefore, we call this model a lump kinetics model. This model is evaluated using the experimental data from the leaching process of laterite ore using a solution of citric acid ($C_6H_8O_7$) at low concentrations. The citric acid solutions at low concentrations are used as solvents because these solutions can be produced through the fermentation pathway of the fungi *Aspergillus niger*.

In the bioleaching process, *Aspergillus niger* has been proven as a leaching media and is able to provide high metal ion recovery results. However, the citric acid produced through the fermentation process is relatively in low concentration. Citric acid is categorized as a weak acid. However, the ability of citric acid to dissociate is high when compared to other organic acids. Furthermore, in previous studies, citric acid showed a better ability to leach metal ions than inorganic acid (sulfuric acid, hydrochloric acid, or nitric acid) [23].

In other words, the developed mathematical model can also be used for the leaching process of metal ions with the help of microorganisms, commonly referred to as the bioleaching process, specifically the bioleaching process using the help of fungi, such as *Aspergillus niger*. In addition, this model is also compared with the simulation results using the shrinking core model.

The Description of the Lump Kinetic Model in the Leaching Process

As mentioned before, the mechanism of the leaching process involves three main steps. Each step has a role as resistance. Consequently, when a solvent is transported from a bulk solution to the surface of an unreacted zone for a reactive extraction process, a decrease in the solvent concentration occurs. It is illustrated in Figure 1. The effect of the number of steps involved in the process needs to be considered in the kinetic study of this process. It is very different from the concept of the shrinking core model, which only considers one step. When one step is involved, the shrinking core model will assume that the other steps take place at a rapid rate, so that the decrease of the solvent concentration can be ignored.

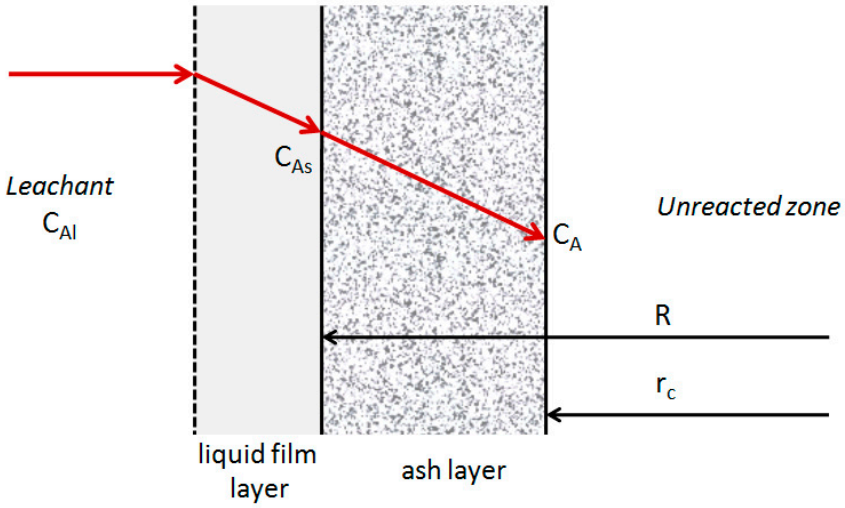

Figure 1. Illustration of the lump kinetic model development.

In the solvent diffusion step from the bulk solution to the surface of solids through the liquid film layer, the applicable mathematical equation is [24]:

$$N_{A,1} = k_c(C_{Al} - C_{As}), \tag{1}$$

where $N_{A,1}$ is the rate of mass transfer of the solvent through the liquid film layer (mole of solvent/area/time); k_c is the mass transfer coefficient (length/time); C_{Al} is the solvent concentration in the bulk solution (mole of solvent/volume); and C_{As} is the solvent concentration on the surface of solids (mole of solvent /volume). Fick's law applies at the step of diffusion of solvents in solids, and the equation is [25–27]:

$$N_{A,2} = -D_e \frac{dC_A}{dr} \tag{2}$$

where $N_{A,2}$ is the mass transfer rate of the solvent in the solid (mole of solvent/area/time); D_e is an effective diffusivity coefficient (area/time); $\frac{dC_A}{dr}$ is the change in the concentration of the solvent with respect to the change in the radius of the solid. Assuming that a chemical reaction runs in order 1, the equation that applies to the step of a chemical reaction is [28]:

$$(-r_A) = k_r C_A \tag{3}$$

where $(-r_A)$ is the reaction rate (mole of solvent/volume/time); k_r is the reaction constant (time^{-1}); and C_A is the solvent concentration (mole of solvent/volume).

In a steady-state at each step in which the unit is equalized into a mole of solvent/time of Equations (1)–(3), the equation expressing the overall process rate is:

$$N_A = \frac{4\pi C_{Al}}{\frac{3}{k_r\, r_c^3} + \frac{1}{D_e}\left(\frac{1}{R_p} - \frac{1}{r_c}\right) + \frac{1}{k_c\, R_p^2}} \tag{4}$$

where N_A, r_c, and R_p are the overall process rate, the radius of the unreacted zone, and the radius of the particles, respectively. Equation (4) can be simplified for the calculation process using an assumption where the solvent diffusion step through the liquid film layer can be ignored. It can be applied in this

process because the leaching process takes place using rapid stirring. This results in thinning of the film layer and the film layer can be considered missing. Thus, Equation (4) becomes:

$$N_A = \frac{4\pi C_{Al}}{\frac{3}{k_r\, r_c^3} + \frac{1}{D_e}\left(\frac{1}{R_p} - \frac{1}{r_c}\right)} \tag{5}$$

The next step is to arrange the solvent mass balance equation in the batch reactor, and by substituting Equation (5) and the equation for the relationship between the extraction recovery fraction of the extracted metal ion (x) to the ratio of the radius of the unreacted zone and the radius of the solid, the formed equation is:

$$\frac{dx}{dt} = \left[\alpha \cdot \frac{1}{(1-x)} + \beta \cdot \frac{\left\{(1-x)^{\frac{1}{3}} - 1\right\}}{(1-x)^{\frac{1}{3}}}\right]^{-1} \tag{6}$$

with:

$$\alpha = \frac{a\, \rho_B}{b\, M_B\, C_{Al}\, k_r} \tag{7}$$

$$\beta = \frac{\alpha\, \rho_B\, R_P^2}{3b\, M_B\, C_{Al}\, D_e} \tag{8}$$

where x is the fraction of metal ion recovery; a and b are stoichiometric constants; ρ_B is solid density; and M_B is the molecular weight of the metal ions. Equations (6)–(8) is the equation that will be evaluated against the experimental data. Detailed explanation of the lump model is presented in the Appendix A.

2. Materials and Methods

Limonite type laterite ores were used in this study. These ores were mined from a mining area in Pomalaa, Indonesia. First, the raw materials were analyzed for the metal content contained therein by S2 Ranger, Bruker X–ray fluorescence (XRF) (Bruker Corporation, Billerica, MA, USA). The results of the analysis are presented in Table 1.

Table 1. Results of X–ray fluorescence (XRF) laterite ore testing.

Element	Fe	Si	Mg	Ni	Al	Cr	Mn	Co
Composition, wt%	26.0	15.5	9.8	2.7	2.5	1.0	0.5	0.1

The leaching process of laterite ore is carried out using a solvent in the form of a solution of citric acid ($C_6H_8O_7$) with a low concentration, which is 0.1 M. This study used a three-neck flask as an extractor, equipped with a water bath, condenser, stirrer, and thermometer. The 300 mL of solvent was poured into the flask and then was heated until it reached the desired temperature, i.e., 303, 333, and 358 K. This operating temperature is chosen to limit the amount of water evaporation and to make the flask easy to handle. Laterite ore powder with a size of 125–150 µm and a quantity up to 60 g was prepared. After the operating temperature was achieved, the powder was put into a flask. Samples to be analyzed were taken from the flask at 0, 1, 2, 5, 10, 15, 30, 60, and 120 min. Each sample was separated between solid and liquid phases using a centrifuge at 1000 rpm for 10 min. The liquid phase was then taken and the metal element concentration was analyzed using Optima 8300, Perkin Elmer inductively coupled plasma-optical emission spectroscopy (ICP-OES) (Perkin Elmer, Waltham, MA, USA). The concentration of metal elements contained in the liquid samples would be used to evaluate the shrinking core and lump models.

3. Results and Discussion

The evaluation of the kinetics model in this study was carried out using experimental data from the leaching process of laterite ores, where the temperature parameters were varied. The temperature has an essential role in the leaching process because it affects the rate of the leaching process, both the diffusion rate and the reaction rate. The results of this experiment are presented in Figure 2.

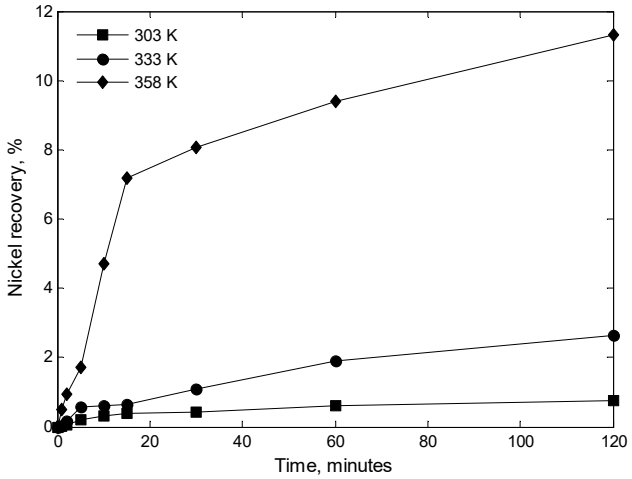

Figure 2. The effect of temperature on the the laterite ore leaching process.

Based on Figure 2, the trend of the percentage of nickel recovery during the extraction time experienced a significant increase, especially at a temperature of 358 K. This shows that the leaching process is strongly influenced by temperature. The increase in temperature causes kinetic energy also to increase so that the probability of collision between molecules will become more frequent. As a result, the diffusion rate of each molecule and the reaction rate will also be faster. In addition, the leaching time also shows an effect where the longer the leaching time was used, the higher the percentage of nickel recovery was reached. This phenomenon is caused by collision factors that often occur along with the length of time leaching.

In this present work, the experimental results, which are shown in Figure 2, will be evaluated using the lump kinetic model. Equations (6)–(8) was applied to simulate that experimental data and the simulation result is presented in Figure 3. Figure 3 shows that there is a relevant result to describe the physical phenomenon, which is happening in the leaching process of nickel laterite using citric acid as a solvent.

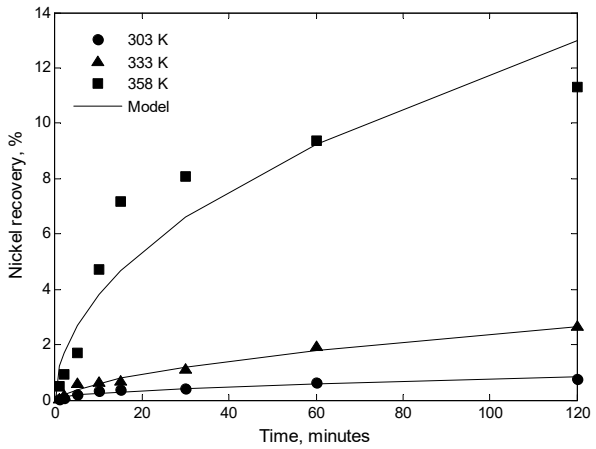

Figure 3. Simulation results using the lump kinetic model.

To compare this simulation, the reactant diffusion-controlled shrinking core model was simulated using the same experimental data, as shown in Figure 2. This model was used because, based on the previous study by [29–31], the most suitable of the shrinking core model was applied when a diffusion reactant through the ash layer controls the leaching process. The simulation of the shrinking core model follows the equation [22,30,32]:

$$k_d \cdot t = 1 - 3(1 - x)^{0.67} + 2(1 - x) \quad (9)$$

where x is the fraction of metal ion recovery, and k_d is the rate constant of the leaching process. The simulation results using the shrinking core model are presented in Figure 4.

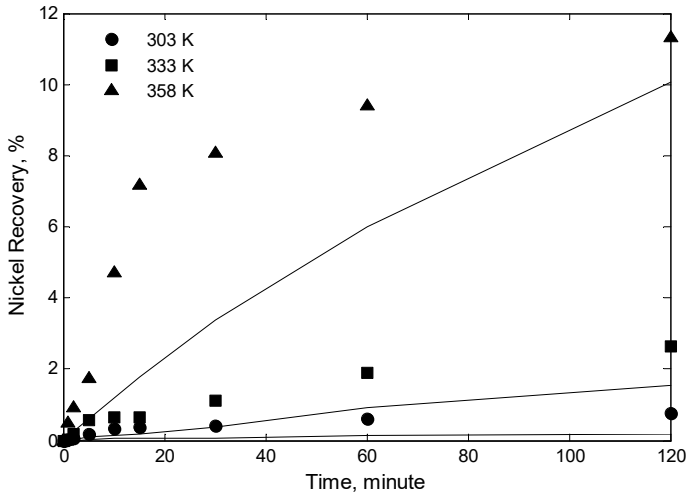

Figure 4. Simulation results using the reactant diffusion-controlled shrinking core model.

Based on Figure 4, the reactant diffusion-controlled shrinking core model has not been able to describe a physical phenomenon that happens in the leaching process of laterite ore using a low concentration of a citric acid solution as a solvent. This simulation result also proves that the lump kinetic model (Figure 3) is a model which can give better simulation results. Quantitatively, the compatibility of the two models can be compared through the percentage of errors from both models. This value shows how big the error of the simulation data is against the experimental data. The error value is calculated using this following equation:

$$\%E = \frac{|C_d - C_s|}{C_d} x \times 100\% \quad (10)$$

where $\%E$ is the percentage of errors; C_d is the concentration of experimental data; and C_s is the concentration of simulation data. The calculation results are presented in Table 2.

Table 2. The percentage of average error from the shrinking core and lump models.

Temperature, K	The Percentage of Average Error, %	
	Shrinking Core Model	Lump Model
303	196.97	51.35
333	108.89	29.39
358	119.74	40.09
The average value	141.86	40.28

The results of calculations that have been carried out and presented in Table 2 show that the simulation process using the shrinking core model gives an average percentage error 3.5 times larger

than that from the simulation process using the lumped model. This condition proves that the assumption of the shrinking core model that only involves one controlling step does not apply in the leaching process of laterite ore using a low concentration of the citric acid solution. The reactant diffusion in a solid step is not the only step that controls the leaching process; the chemical reaction step in the unreacted core also has a significant role in this process.

Figure 2 reinforces the presence of more than one factor that controls the leaching process: the trend graphs show that during the leaching process there are two trends that indicate the diffusion step and the chemical reaction step affect each other, primarily when the leaching process was carried out at 358 K. In the first 10 min of the leaching process the percentage increase in nickel recovery was quite sharp. This phenomenon indicates that the leaching process is affected by the step of chemical reactions in the surface particles. Citric acid solvents will react first with nickel oxide (NiO) compounds that are on the surface of solids, and it can be said that there has not yet been a diffusion step in solids or is usually called internal diffusion. However, after the leaching process has been running for more than 10 min, the profile of the increased nickel recovery percentage is not too sharp; this indicates that the internal diffusion step has begun to affect the leaching process.

Therefore, this simulation process indicates that the shrinking core model is not very suitable for modeling the metal leaching process. In addition, the leaching process is done using organic acids, such as citric acid and acetic acid. The use of organic acids will produce products containing complex metals (ligands), which have a large enough molecule diameter. This condition will affect the rate of internal diffusion, which slows down due to the jostling between the reactant molecules and the product molecules (the reactant molecules enter the solid while the product molecules exit the reactants). Another study conducted by [33] supports the results of this simulated study. In its study, the conventional shrinking core model was also unable to match experimental data from the cobalt leaching process from a spent battery using an acetic acid solution. Another condition that causes a mismatch of the shrinking core model is reversible chemical reactions. The reversible chemical reaction conditions will occur in the reaction of the metal compounds with an organic acid solution.

In this study, the lumped model was evaluated under certain conditions where acid concentration, operating temperature, and percentage of metal ion recovery were low. However, the use of this model can still be applied to different leaching process conditions, for example, high acid concentrations, high operating temperatures, or a high percentage of metal ion recovery. This can occur because the development of the lumped model is based on the mechanism that occurs in the leaching process using organic acids. The basis for developing a lumped model is more complex than the shrinking core model, therefore the lumped model is more versatile at all conditions of the leaching process.

Although the lump kinetic model is a better model than the shrinking core model, Figure 3 and Table 2 also show that the lump kinetic model still can be improved. It indicates that there is another step that controls the leaching process using a citric acid solution. For example, product diffusion control through the ash layer is predicted to have a role in this process. It can be considered because nickel citrate, which is a complex compound (ligand) is formed. This compound has a large molecule size and will obstruct the diffusion path. Therefore, another study is needed to prove that allegation.

4. Conclusions

The kinetics study of the leaching process is essential in order to scale up a process from a laboratory scale to an industrial scale. In the leaching process of laterite ore using a low concentration of the citric acid solution, the operating temperature has an important role in the process, especially in terms of the rate of diffusion and the rate of chemical reactions. The experimental results show that the higher the operating temperature used, the higher the percentage of nickel recovered. This experimental data is used to evaluate the shrinking core kinetics model and the lumped model. Simulation results show that the shrinking core model is not able to illustrate the real phenomenon of the leaching process. Based on the average error percentage, the shrinking core model gives a result 3.5 times greater than that of the lumped model. This condition indicates that the leaching process can not be represented by

only one step in the control process. This study proves that the step of internal diffusion and the step of chemical reactions control the leaching process simultaneously.

Author Contributions: Conceptualization, methodology, software, and validation K.C.W., I.P., and H.T.B.M.P.; methodology, K.C.W., I.P., and H.T.B.M.P.; formal analysis, K.C.W. and W.A.; investigation, K.C.W.; resources, W.A.; writing—original draft preparation, K.C.W.; writing—review and editing, I.P. and H.T.B.M.P.; visualization, K.C.W.; supervision, I.P. and H.T.B.M.P. All authors have read and agreed to the published version of the manuscript.

Funding: This research received no external funding.

Acknowledgments: The authors would like to thank the Department of Chemical Engineering, Universitas Gadjah Mada because of the analysis equipment support and the Indonesian Institute of Sciences (LIPI) because of material support.

Conflicts of Interest: The authors declare no conflict of interest.

Appendix A

The mechanism of the leaching process using organic acid is illustrated in Figure 1 and it is controlled by three steps, i.e., the solvent diffusion step from the bulk solution to the surface of solids through the liquid film layer, the solvent diffusion step in solid, and the chemical reaction steps. Equations (1)–(3) are the mathematical equations which describe the three controlling steps in the leaching process. If the leaching process runs in a steady-state condition, then the rate of each controlling step can be considered in a same condition. Therefore, Equations (1)–(3) need to be adjusted, so the unit of each equation becomes mole of solvent/time. Equations (1)–(3) change to the following equation.

$$N_{A,1} = k_c(C_{Al} - C_{As})4\pi R_p^2 \tag{A1}$$

$$N_{A,2} = {}^{4\pi D_e\,(C_{As}-C_A)}\Big/\left(\frac{1}{R_p} - \frac{1}{r_c}\right) \tag{A2}$$

$$(-r_A) = k_r\, C_A\, \frac{4}{3}\pi r_c^3 \tag{A3}$$

When $N_{A,1}$, $N_{A,2}$, and $(-r_A)$ are in same condition (steady-state), the overall process rate can be expressed in Equation (4). Equation (4) can be simplified for the calculation process using an assumption where the solvent diffusion step through the liquid film layer can be ignored. It can be applied in this process because the leaching process takes place using rapid stirring. This results in thinning of the film layer and the film layer can be considered missing. Thus, Equation (4) becomes:

$$N_A = \frac{4\pi C_{Al}}{\frac{3}{k_r\, r_c^3} + \frac{1}{D_e}\left(\frac{1}{R_p} - \frac{1}{r_c}\right)} \tag{A4}$$

The solvent mass balance equation in the batch reactor is developed as follows.

$$\text{Rate of input} - \text{Rate of output} = \text{Rate of accumulation n (mole of solvent /time)} \tag{A5}$$

$$0 - 4\pi C_{Al}\left[\frac{3}{k_r\, {r_c}^3} + \frac{1}{D_e}\left(\frac{1}{R_p} - \frac{1}{r_c}\right)\right]^{-1} = \frac{dN_A}{dt} \tag{A6}$$

$$0 - 4\pi C_{Al}\left[\frac{3}{k_r\, {r_c}^3} + \frac{1}{D_e}\left(\frac{1}{R_p} - \frac{1}{r_c}\right)\right]^{-1} = \frac{a}{b}\,\frac{dN_B}{dt} \tag{A7}$$

$$-4\pi C_{Al}\left[\frac{3}{k_r\, {r_c}^3} + \frac{1}{D_e}\left(\frac{1}{R_p} - \frac{1}{r_c}\right)\right]^{-1} = \frac{a}{b}\,\frac{d}{dt}\left(\rho_B \frac{4}{3}\,\pi\, {r_c}^3\,\frac{1}{M_B}\right) \tag{A8}$$

$$-C_{Al}\left[\frac{3}{k_r\, {r_c}^2} + \frac{1}{D_e}\left(\frac{r_c}{R_p} - 1\right)\right]^{-1} = \frac{a}{b}\,\frac{\rho_B}{M_B}\, r_c\,\frac{dr_C}{dt} \tag{A9}$$

Variable r_c and R_p have a relation with the fractional conversion and can be expressed as follows [32].

$$\frac{r_c}{R_p} = (1-x)^{1/3} \tag{A10}$$

$$\frac{dr_c}{dt} - \frac{R_p}{3}(1-x)^{-2/3}\frac{dx}{dt} \tag{A11}$$

By substituting Equation (A11) to Equation (A9), the equation becomes as follows:

$$\frac{dx}{dt} = \left[\alpha \cdot \frac{1}{(1-x)} + \beta \cdot \frac{\left\{(1-x)^{1/3} - 1\right\}}{(1-x)^{1/3}}\right]^{-1} \tag{A12}$$

with:

$$\alpha = \frac{a\,\rho_B}{b\,M_B\,C_{Al}\,k_r} \tag{A13}$$

$$\beta = \frac{\alpha\,\rho_B\,R_P^2}{3b\,M_B\,C_{Al}\,D_e} \tag{A14}$$

Equations (A12)–(A14) is the equation that will be evaluated against the experimental data.

References

1. Abas, N.; Kalair, A.; Khan, N. Review of fossil fuels and future energy technologies. *Futures* **2015**, *69*, 31–49. [CrossRef]
2. Ellabban, O.; Abu–Rub, H.; Blaabjerg, F. Renewable energy resources: Current status, future prospects and their enabling technology. *Renew. Sustain. Energy Rev.* **2014**, *39*, 748–764. [CrossRef]
3. Ponrouch, A.; Frontera, C.; Bardé, F.; Palacín, M.R. Towards a calcium–based rechargeable battery. *Nat. Mater.* **2015**, *15*, 169–172. [CrossRef] [PubMed]
4. Goodenough, J.B.; Park, K.S. The Li–ion rechargeable battery: A perspective. *J. Am. Chem. Soc.* **2013**, *135*, 1167–1176. [CrossRef] [PubMed]
5. Kularatna, N. Rechargeable batteries and their management. *IEEE Instrum. Meas. Mag.* **2011**, *14*, 20–33. [CrossRef]
6. Palacín, M.R. Recent advances in rechargeable battery materials: A chemist's perspective. *Chem. Soc. Rev.* **2009**, *38*, 2565–2575. [CrossRef]
7. Ruetschi, P.; Meli, F.; Desilvestro, J. Nickel–metal hydride batteries. The preferred batteries of the future? *J. Power Sources* **1995**, *57*, 85–91. [CrossRef]
8. Yang, Y.; McDowell, M.T.; Jackson, A.; Cha, J.J.; Hong, S.S.; Cui, Y. New nanostructured Li_2S/silicon rechargeable battery with high specific energy. *Nano Lett.* **2010**, *10*, 1486–1491. [CrossRef]
9. Gao, X.P.; Yao, S.M.; Yan, T.Y.; Zhou, Z. Alkaline rechargeable Ni/Co batteries: Cobalt hydroxides as negative electrode materials. *Energy Environ. Sci.* **2009**, *2*, 502–505. [CrossRef]
10. Liu, Z.; Tay, S.W.; Li, X. Rechargeable battery using a novel iron oxide nanorods anode and a nickel hydroxide cathode in an aqueous electrolyte. *Chem. Commun.* **2011**, *47*, 12473–12475. [CrossRef]
11. Han, S.C.; Kim, K.W.; Ahn, H.J.; Ahn, J.H.; Lee, J.Y. Charge-discharge mechanism of mechanically alloyed NiS used as a cathode in rechargeable lithium batteries. *J. Alloy. Compd.* **2003**, *361*, 247–251. [CrossRef]
12. Shukla, A.K.; Venugopalan, S.; Hariprakash, B. Nickel-based rechargeable batteries. *J. Power Sources* **2001**, *100*, 125–148. [CrossRef]
13. Bhargava, S.K.; Pownceby, M.I.; Ram, R. Hydrometallurgy. *Metals* **2016**, *6*, 122. [CrossRef]
14. Aarabi–Karasgani, M.; Rashchi, F.; Mostoufi, N.; Vahidi, E. Leaching of vanadium from LD converter slag using sulfuric acid. *Hydrometallurgy* **2010**, *102*, 14–21. [CrossRef]
15. Ajemba, R.O.; Onukwuli, O.D. Application of the shrinking core model to the analsys of alumina leaching from Ukpor clay using nitric acid. *Int. J. Eng. Res. Technol.* **2012**, *1*, 1–13.
16. Ayanda, O.S.; Adekola, F.A.; Baba, A.A.; Fatoki, O.S.; Ximba, B.J. Comparative study of the kinetics of dissolution of laterite in some acidic media. *J. Miner. Mater. Charact. Eng.* **2011**, *10*, 1457–1472. [CrossRef]

17. Feng, X.L.; Long, Z.Q.; Cui, D.L.; Wang, L.S.; Huang, X.W.; Zhang, G.C. Kinetics of rare earth leaching from roasted ore of bastnaesite with sulfuric acid. *Trans. Nonferrous Met. Soc. China* **2013**, *23*, 849–854. [CrossRef]
18. Gharabaghi, M.; Irannajad, M.; Azadmehr, A.R. Leaching kinetics of nickel extraction from hazardous waste by sulphuric acid and optimization dissolution conditions. *Chem. Eng. Res. Des.* **2013**, *91*, 325–331. [CrossRef]
19. Huang, J.; Chen, M.; Chen, H.; Chen, S.; Sun, Q. Leaching behavior of copper from waste printed circuit boards with Brønsted acidic ionic liquid. *Waste Manag.* **2014**, *34*, 483–488. [CrossRef]
20. Olanipekun, E.O. Kinetics of leaching laterite. *Int. J. Miner. Process.* **2000**, *60*, 9–14. [CrossRef]
21. Wang, Y.; Jin, S.; Lv, Y.; Zhang, Y.; Su, H. Hydrometallurgical process and kinetics of leaching manganese from semi-oxidized manganese ores with sucrose. *Minerals* **2017**, *7*, 27. [CrossRef]
22. Wanta, K.C.; Perdana, I.; Petrus, H.T.B.M. Evaluation of shrinking core model in leaching process of Pomalaa nickel laterite using citric acid as leachant at atmospheric conditions. *IOP Conf. Series Mater. Sci. Eng.* **2016**, *162*, 012018. [CrossRef]
23. Astuti, W.; Hirajima, T.; Sasaki, K.; Okibe, N. Comparison of effectiveness of citric acid and other acids in leaching of low-grade Indonesian saprolitic ores. *Miner. Eng.* **2016**, *85*, 1–16. [CrossRef]
24. Geankoplis, C.J. *Transport Processes and Unit Operation*, 3rd ed.; Prentice-Hall International Editions: Upper Saddle River, NJ, USA, 1993; p. 385.
25. McCabe, W.L.; Smith, J.C.; Harriott, P. *Unit Operations of Chemical Engineering*, 5th ed.; McGraw-Hill International Editions: Singapore, 1993; p. 650.
26. Berk, Z. Chapter 3—Heat and mass transfer, basic principles. In *Food Process Engineering and Technology*; Academic Press: Cambridge, MA, USA, 2018; pp. 79–126.
27. Liang, Y. *Diffusion in Encyclopedia of Geochemistry*; Springer International Publising: Berlin/Heidelberg, Germany, 2018; pp. 1–13.
28. Fogler, H.S. *Elements of Chemical Reaction Engineering*, 4th ed.; Prentice Hall Professional Technical Reference: Upper Saddle River, NJ, USA, 2006; p. 83.
29. Wang, X.; Srinivasakannan, C.; Duan, X.H.; Peng, J.H.; Yang, D.J.; Ju, S.H. Leaching kinetics of zinc residues augmented with ultrasound. *Sep. Purif. Technol.* **2013**, *115*, 66–72.
30. Astuti, W.; Hirajima, T.; Sasaki, K.; Okibe, N. Kinetics of nickel extraction from Indonesian saprolitic ore by citric acid leaching under atmospheric pressure. *Miner. Metall. Process.* **2015**, *32*, 176–185. [CrossRef]
31. Agacayak, T.; Zedef, V.; Aras, A. Kinetic study on leaching of nickel from Turkish lateritic ore in nitric acid solution. *J. Cent. South Univ.* **2016**, *23*, 39–43. [CrossRef]
32. Levenspiel, O. *Chemical Reaction Engineering*, 3rd ed.; John Wiley & Sons, Inc.: New York, NY, USA, 1999; pp. 570–576.
33. Setiawan, H.; Petrus, H.T.B.M.; Perdana, I. A kinetics study of acetic acid on cobalt leaching of spent LIBs: Shrinking core model. *MATEC Web Conf.* **2018**, *154*, 01033. [CrossRef]